ORIGINAL PAPER

Construction of an Off-On Fluorescence System Based on Carbon Dots for Trace Pyrophosphate Sensing

Qiaoli Yue · Yining Hou · Shuzhen Yue · Kaimin Du ·
Tongfei Shen · Lei Wang · Shuling Xu · Haibo Li ·
Jifeng Liu

Abstract A novel and simple fluorescence Off-On system is proposed for selective pyrophosphate (PPi) sensing in an aqueous solution. The method is constructed based on the strong blue emission of carbon dots (CDs) owing to its outstanding photoluminescence and easy synthesis, which has shown exciting potential in analytical and biological field. The fluorescence of CDs can be remarkably quenched by some transition metal ions such as Cu^{2+}, Ni^{2+}, Mn^{2+} and Co^{2+} due to the coordination reaction between metal ions and the carboxylic groups on the surface of CDs. When PPi was introduced to CDs-metal ion system the fluorescence of CDs was recovered regularly. The increment of fluorescence intensity was proportional with the concentration of PPi in the range of 1–200 μM and correspondingly the limit of detection was calculated as 0.32 μM according to the recommendation of IUPAC as 3.29 S_B/m. The possible mechanism was discussed for the detection of PPi and the quenching reaction between CDs and metal ions. Furthermore, the proposed system was successfully used to monitor the content of PPi in water samples from artificial wetland.

Keywords Pyrophosphate · Carbon dots · Transition metal ion · Fluorescence quenching

Introduction

The use of nanomaterials for the development of chemosensors has been explored over the past two decades,

Q. Yue (✉) · Y. Hou · S. Yue · K. Du · T. Shen · L. Wang · S. Xu ·
H. Li · J. Liu (✉)
Department of Chemistry, Liaocheng University,
Liaocheng 252059, China
e-mail: qiaoli_yue@hotmail.com
e-mail: liujifeng111@gmail.com

due to the unique optical, electronic, and magnetic properties [1]. These sensors based on nanomaterials open up a new avenue for simple, sensitive, on-site analysis of specific targets. Fluorescent semiconductor quantum dots (QDs) have been found wide applications in bioimaging and biomedicine [2]. However, these popular QDs have serious toxicity even at relatively low concentrations [3]. Therefore, development of nanoparticles free of cadmium (Cd), lead (Pb), and mercury (Hg) is important and urgent due to the environmental hazard for biological and photovoltaic applications for such toxic materials [4]. It was reported that carbon dots (CDs) possessed a high quantum yields (QY, ~60 %), nontoxicity, nonblinking, low photobleaching, high photostability, and large two-photon cross-section [5, 6].

CDs are a kind of newly emerging fluorescent nanomaterials with sizes below 10 nm, first obtained during purification of single-walled carbon nanotubes through preparative electrophoresis in 2004 [7]. CDs have generated enormous excitement because of their superiority in water solubility, chemical inertness, low toxicity, ease of functionalization and resistance of photobleaching [8]. The main reason why such tiny CDs have recently attracted wide attention is because of their strong fluorescence, for which they are referred to as fluorescent carbon. The possible mechanism for the fluorescence emission of CDs is attributed to radioactive recombinations between the trapped electrons and holes on the surface of CDs [6, 9], based on the decoration with a variety of oxygenated species including carboxylic, lactonic, and phenolic moieties on the CDs particle surface [10]. Despite the progress, the fundamental mechanism of the CDs photoluminescence remains largely unknown. Although the exact mechanisms responsible for fluorescence in CDs, especially blue to ultraviolet emission, remain to be elucidated, the intrinsic fluorescence of CDs in the visible and NIR range makes it attractive for numerous applications [11]. CDs have been used to determine many substances including

biomolecules such as DNA [12], thrombin [13], biothiol [14], glucose [15], inorganic anions including PO_4^{3-} [16], free chlorine [17], and NO_2^- [18], and metal ions Ag^+ [19], and Hg^{2+} [20]. For the applications of CDs, the quenching effect of analyte on the fluorescence of CDs was widely used especially for metal ions.

Pyrophosphate (PPi) is essential to life processes, and understanding their hydrolysis and related phosphoryl transfer, involving cleavage within a P-O-P framework, is of recognized importance [21]. In biological systems, PPi are produced by a number of biochemical reactions, such as ATP hydrolysis, DNA and RNA polymerizations cyclic AMP formation by the enzyme adenylate polymerizations, cyclase, and the enzymatic activation of fatty acids to form their coenzyme A esters. Many pathological disorders such as familial chondrocalcinosis are associated with abnormal regulation of the transport of inorganic PPi [22]. In this case, various optical technologies were developed for PPi detection. For instance, luciferase-based PPi detection was used for bacterial detection and DNA sequencing applications [23]. Non-enzymatic methods were also reported for the determination of PPi [24, 25]. The fluorescence- and absorption-based detection using PPi chelators can detect submicromolar PPi in bulk solution. In one way, PPi was detected using fluorescence methods based on the coordination interaction of PPi on the structure of metal complex or ligand including zinc complex [26–28], dimethyltin (IV)–alizarin red S complex [29], copper complex [30], thulium complex [31], single-stranded-DNA–Al (III) complex [32], and di-(2-picolyl)amine resulted in the "turn-on" effect of the system, named chelation-based sensing. Among the metal-complex-based receptors, the ones that exhibit fluorescence enhancement in the presence of Zn^{2+} have attracted considerable attention because of the strong affinity of Zn^{2+} toward phosphates. In other way, the chelator is designed which can bind to indicator dyes, where Ppi is detected either fluorescently [33] or electrically [34] when dye molecules are displaced from chelator by PPi binding.

Considering all of these issues, herein, for the first time, we report an unmodified CDs fluorescent sensor based on the fluorescence quenching of transition metal ions for the detection of PPi with high sensitivity and selectivity. We presented a facile route to synthesize fluorescent CDs which have great amounts of hydroxyls without complicated separation and further modification of the surface (Scheme 1). The quantum yield (QY) of the product can reach 9.9 %, which is higher than those CDs reported previously [35–39]. It was supposed that hydroxyls have strong electron donated ability, which benefit the fluorescence emission, while carboxyls have strong electron drawing ability with the opposite effect, thus the fluorescence properties of hydroxyls-coated CDs are better than those carboxyls-coated [11]. Furthermore, the fluorescence signals of the as-prepared CDs are stable for more than 5 months at 4 °C.

As described above, PPi is usually chelated with metal ions to form coordination complexes. In addition, coordination chemistry of Cu^{2+} is dominated by nitrogen- or oxygen-donating ligands due to Cu^{2+} being classified as a borderline hard acid [40]. Therefore, an off-on fluorescent system was recommended to the assay of PPi based on the strong fluorescence of CDs and two pairs of coordination reactions for which one is between hydroxyls on CDs and some transition metal ions like Cu^{2+}, and the other is between Cu^{2+} and PPi (Scheme 1).

Experimental Section

Materials

Glyoxal (Sigma-Aldrich, St. Louis, MO) was tested as carbon source and alcohol was tried for the synthesis of CDs. Cu^{2+}, Ni^{2+}, Mn^{2+} and Co^{2+} were all in hydrocholoric acid salts such as $CuCl_2 \cdot 2H_2O$ (Sigma), $NiCl_2$ (Aldrich), $MnCl_2$ (Sigma) and $CoCl_2 \cdot 6H_2O$ (Sigma) used for the fluorescence quenching test of CDs. The following compounds were employed for assessing the selectivity of the sensing approach: Na_3PO_4, NaH_2PO_4, Na_2HPO_4, $Na_2S_2O_3$, Na_2SO_4, NaI, $NaHCO_3$, $NaNO_3$, Na_2SO_3, CH_3COONa, $NaIO_3$, $NaBr$, NaF, Na_2S, $NaNO_2$, $Na_2S_2O_8$, and $NaClO_3$ obtained from Beijing Chemical Works (Beijing, China). A 1.0 mM stock solution of $P_2O_7^{4-}$ was prepared from $Na_4P_2O_7 \cdot 10H_2O$, which was purchased from Sigma-Aldrich. Working solutions were prepared by dilution of the stock solution as required. Ultrapure water (≥18.2 MΩ) used throughout the experiment was obtained from the double distilled water deionized by a Millipore system and all chemicals were at least analytical reagent grade.

Scheme 1 Schematic illustration of the interaction mechanism between CDs and Cu^{2+} and the recovery fluorescence of CDs by PPi
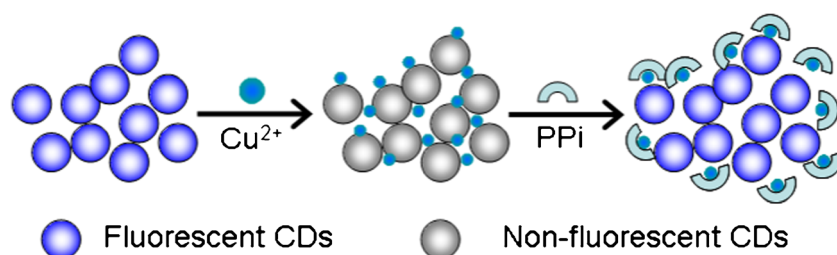
Apparatus and Characterization

The morphology of the samples was obtained from transmission electron microscopy (TEM) observations, which were performed on a JEM 2100 electron microscope (JEOL, Japan) operating with a 200 kV acceleration voltage. Samples for TEM were prepared by placing a drop of the suspension on the carbon-coated copper grid. Fourier transform infrared (FT-IR) spectra were recorded on an IR2000 Nicolet FT-IR spectrometer within the range of 400–4000 cm^{-1}. Absorption spectra of samples were collected using a Lambda 25 UV–vis spectrophotometer (Perkin Elmer, USA). The fluorescence measurements were performed on an F-7000 spectrophotometer (Hitachi Co. Ltd., Japan) with a common 10 mm slit sample cell. The portable instrument is well suited to field analysis since it only requires connection through a USB to a computer.

Synthesis of CDs

CDs were prepared by a little modified prior method [41]. Briefly, glyoxal (5 ml) was dispersed in 20 ml ethanol. Before the system was ultrasonicated for 10 min to ensure the formation of a homogeneous suspension, the pH of the solution was adjusted to ca. 8 with 0.5 M NaOH under vigorously stirring. Subsequently, the suspension was transferred into a 50 ml poly(tetrafluoroethylene) (Teflon)-lined stainless-steel autoclave, and additional ethanol was added until the vessel was 80 % full. The autoclave sealed was heated at 140 °C for 4 h. After cooling to room temperature, the resulting black suspension was filtered through a 0.22 μm microporous membrane and a brown filter solution (yield ca. 22 %) was separated. The colloidal solution still contained some large particles that emitted weak blue fluorescence. Thus, the colloidal solution was further dialyzed in a dialysis bag (retained molecular weight: 3500 Da) overnight and CDs that were strongly fluorescent through the bag were obtained with a yield of ca. 12 %.

Determination of the Quantum Yields

To obtain the quantum yield (QY,Φ) of all samples, the procedure was accomplished by comparison of the wavelength integrated intensity of sample to that of the standard quinine sulfate. First of all, the optical density was kept below 0.05 to avoid inner filter effects. The quantum yields of these obtained products were calculated using the following equation.

$$\Phi_x = \Phi_s \left(m_x \big/ m_s \right) \Big/ \left(\eta_x^2 \big/ \eta_s^2 \right)$$

Where Φ is the quantum yield, m is the integrated intensity, and η is the refractive index of the solvent. The subscript x and s refers to the sample and standard reference of known

quantum yield, respectively. Quinine sulfate was chosen as the standard, whose quantum yield is 0.577 and nearly constant for excitation wavelength from 200 to 400 nm. For the determination of quantum yield the slope method was also used to confirm the obtained data [42, 43].

Analysis of PPi

50 μl CDs solution and 1.0 ml Tris–HCl buffer solution (pH 8.0) were added to a 5.0-ml cholorimetric tube. Then 50 μl working solution for one of the metal ions among Cu^{2+}, Ni^{2+}, Mn^{2+} and Co^{2+} was added, the mixture was vortexed thoroughly and incubated for 15 min. Subsequently, the appropriate amount of PPi solution was added, vortex-mixed and placed for another 15 min. At last, the solution was diluted to the total volume of 2.0 ml before the measurements. The fluorescence spectra were recorded at the F-5000 spectrophotometer by fitting the excitation wavelengths at 348.0 nm, during which the spectral bandwidths were kept at 5.0 nm for both exciting and emitting monochromators. Fluorescence intensity was measured at 426.0 nm.

Procedure for the Water Samples

The water samples were obtained from one of the artificial wetlands located at Liaocheng University, China. The three samples for Sample I and II were collected from the entrance and exit of the wetland, respectively. The supernatant of all the water samples were filtered through 0.45 μm membrane after precipitation overnight, then diluted and detected according to the general procedure with five replicates for each sample. In order to evaluate the accuracy of the proposed method, other quantities of standard PPi were added to the samples solution for recovery tests.

Results and Discussion

Characterization

Morphological and Structural Characterizations of CDs The TEM images of the CDs are shown in Fig. 1a, illustrating that the as-prepared CDs are well-dispersed and the CDs were mostly spherical dots. The size distribution ranges from 0.8 to 1.9 nm (inset of Fig. 1a), and average diameter is 1.3 nm (based on statistical analyses of more than 200 dots).

The surface structure and composition of the as-prepared CDs were then investigated. The chemically synthesized CDs were readily water-dispersible due to the presence of suspended hydroxyl and carboxylic groups at the surface, which was confirmed by FT-IR spectroscopy. As shown in Fig. 1b, there were typical peaks around 3440 and 1400 cm^{-1}, which were ascribed to the stretching vibrations

Fig. 1 TEM images (**a**) and FT-IR data (**b**) of CDs
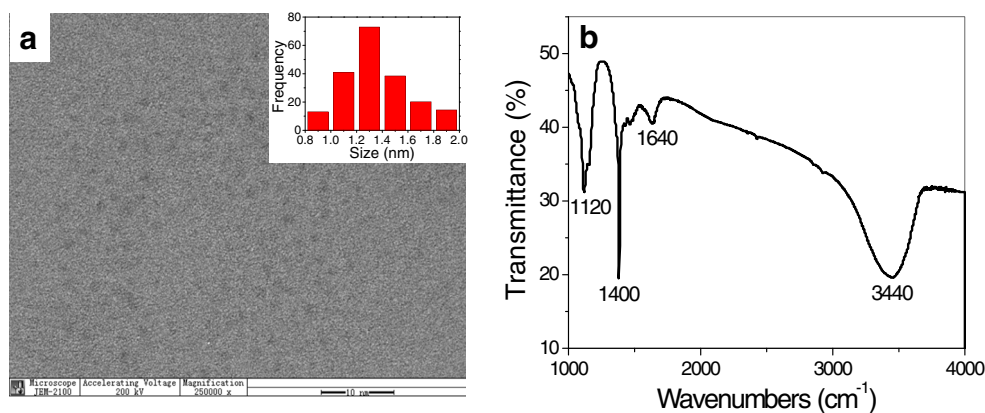
and in-plane bending vibration of –OH, respectively. The dull and intense band of 3440 cm^{-1} indicated the existence of hydrogen bonds, and that at 1640 cm^{-1} manifested the existence of carbonyl (C=O). The band at 1120 cm^{-1} should be ascribed to the stretching vibrations of C-O.

Optical Properties of CDs To explore the optical properties of the CDs, UV–vis absorption and fluorescence spectra were studied. Figure 2a and b is the absorption and fluorescence spectra of CDs in aqueous solution in UV–vis range. From the UV–vis absorption spectrum of CDs (Fig. 2a), there was no obvious peak observed in the UV–vis absorption region. This phenomenon is analogous to the behaviors of the semiconductor quantum dots [16, 36]. Subsequent fluorescence characterization indicated that the CDs can emit strong blue fluorescence under excitation at 365 nm with a UV lamp (Fig. 2b, inset). It can be found from fluorescence spectra that the peak wavelength of excitation and emission was at 348 and 426 nm, respectively (Fig. 2b).

In addition, the QY of CDs is calculated as about 9.9 % with quinine sulfate as a standard reference as described in Experimental Section (Fig. 2c). The result is substantially higher than that of the CDs obtained from various soot species by refluxing with nitric acid followed by complicated separation or modification procedures [17, 36, 38, 39].

Optimal Conditions for PPi Detection

Effect of Excitation Wavelength on the Fluorescence of CDs CDs exhibit an excitation-dependent fluorescence behavior as shown in Fig. 2d. When the excitation wavelength changes from 300 to 410 nm, the fluorescence emission peak

Fig. 2 Excitation (**a**) and emission (**b**) spectra with the peaks at 348 and 426 nm, respectively, the inset of B is the photograph of CDs under UV lamp (365 nm), the integrated fluorescence and absorbance of CDs and quinine sulfate (**c**), ■ quinine sulfate (QS), ● CDs (x), and the fluorescence spectra of the CDs with different excitation wavelengths
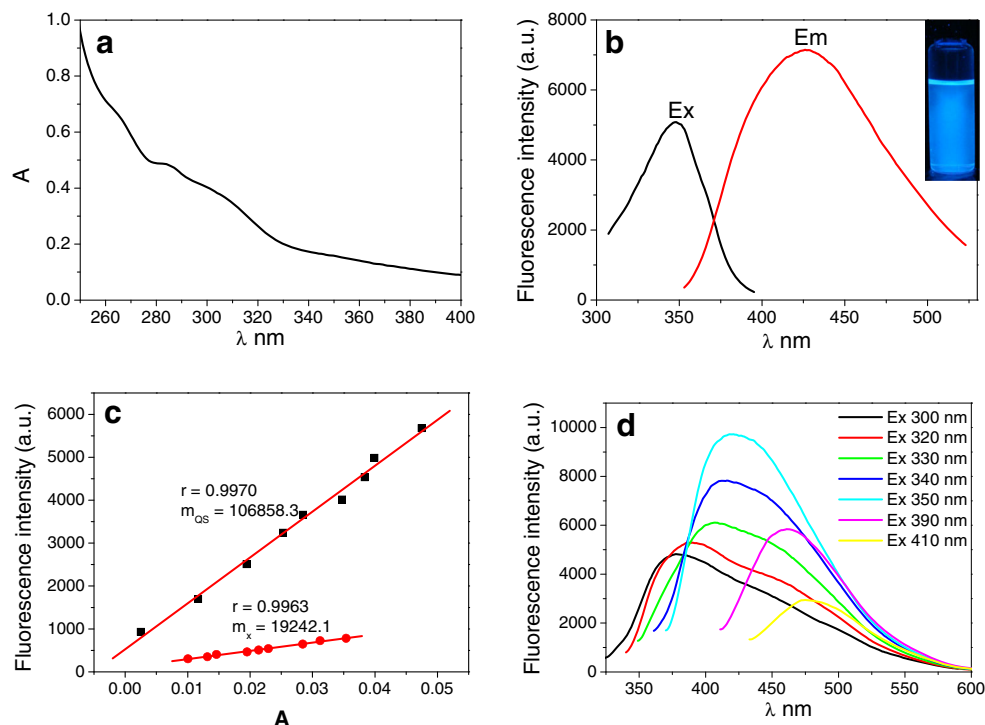
correspondingly shifts from 379 to 476 nm with different intensity. The most intense fluorescence from CDs appears under the 350 nm UV light irradiation and has a maximum at 426 nm. This excitation-dependent fluorescence behavior was extensively reported in fluorescent carbon-based nanomaterials, and it may result from optical selection of differently sized CDs and surface defects of CDs [44, 45]. The CDs have a largely featureless profile absorption, which is consistent with indirect bandgap semiconductor nanomaterials, thus to a certain extent the CDs belong to indirect bandgap semiconductor materials.

Effect of CDs Dosage and Cu^{2+} Concentration In order to obtain a high sensitivity and a wide linear range, the influences of the dosage of CDs and the concentration of Cu^{2+} on the present system were examined. Results show that when a large dose of CDs was used, a higher concentration of Cu^{2+} need be added to achieve an appropriate quenching effect for the determination of PPi. The linear range for PPi was wide but a low sensitivity. On the contrary, a small dosage of CDs was used with a favorable sensitivity but narrow linear range. By consideration of both sensitivity and linear range, 0.01 mg ml^{-1} CDs and 1 μM Cu^{2+} were chosen to detect PPi.

Effect of pH Value and Ion Strength It was reported that the pH of the medium strongly influences the fluorescence of CDs [46, 47], so the study of this variable is critical for the development of the fluorescence assay. First of all, four different buffer solutions including NaH_2PO_4-Na_2HPO_4, NaOAc-HOAc, HCl-$Na_4B_2O_7$, and Tris–HCl were studied in this work. It was found that the ΔF of the system reached a maximum in Tris–HCl buffer solution. Thus, Tris–HCl buffer solution was employed for the following work. Subsequently, the acidity of the detection system was adjusted with Tris–HCl buffer solution. As shown in Fig. 3a, with increase of pH the value of ΔF for detection of PPi reached a maximum at pH 8.0. For this phenomenon, it can be mainly attributed to the stability of PPi and the coordination interaction between PPi and Cu^{2+} [48]. In addition, the effect of pH value on the fluorescence of CDs was not significant in the range of 5–11 (Fig. 3a inset). It can be deduced that for the present product of CDs the surface situation did not change a lot in a wide pH range [17], and therefore the fluorescence intensity hardly changed. Thus, Tris–HCl buffer solution of pH 8.0 was used for the determination of PPi. Furthermore, the stability of CDs fluorescence is hardly influenced by ion strength as illustrated in Fig. 3b.

Interference Effect

The selectivity of the fluorescent probe was evaluated by testing the response of the fluorescent probe to other metal cations under optimum conditions in the case of 100 μM PPi (Fig. 4).
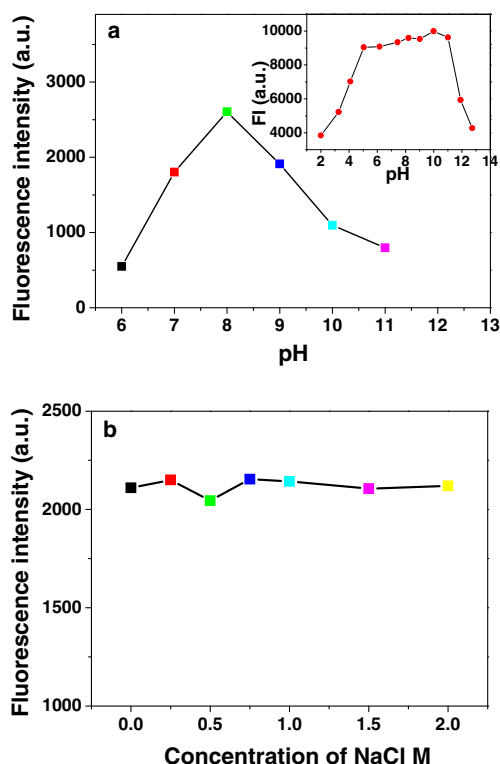

Fig. 3 Effect of ion strength (**a**) and pH (**b**) on the detection of PPi and the fluorescence of CDs (*FI* Fluorescence intensity)

Stock solutions of the respective anions under study were prepared from their sodium salts. When the relative error (Er) exceeded ±5 %, each anion was considered as an interfering agent. From Fig. 4, it can be observed that most anions at high concentration only caused negligible fluorescence change: I_3^-, Br^-, F^-, NO_2^-, and ClO_3^- (100 fold), HPO_4^{2-}, SO_3^{2-}, CH_3COO^-, HCO_3^-, and $H_2PO_4^-$ (50 fold), Ca^{2+}, Mg^{2+}, Zn^{2+}, Fe^{3+}, Cd^{2+}, and Cr^{3+} (30 fold), and PO_4^{3-} (20 fold). The results confirmed an excellent selectivity for the determination of PPi using the present CDs system.
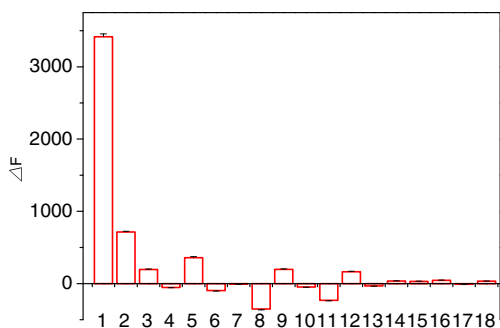

Fig. 4 Fluorescence intensity change upon the addition of different anions (from 1 to 18, the anions tested were $P_2O_7^{4-}$ (1), PO_4^{3-} (2), Ca^{2+} (3), HPO_4^{2-} (4), Mg^{2+} (5), SO_3^{2-} (6), I_3^- (7), Zn^{2+} (8), Fe^{3+} (9), CH_3COO^- (10), Cd^{2+} (11), Cr^{3+} (12), Br^- (13), HCO_3^- (14), F^- (15), $H_2PO_4^-$ (16), NO_2^- (17), and ClO_3^- (18), respectively). The *error bars* represent the results of three separate measurements

Application for PPi Analysis

The calibration curve for PPi detection was carried out under the optimum conditions. As Fig. 5a showed, the relative fluorescence intensity of CDs was regularly recovered with the increase of PPi concentration. Furthermore, the enhancement of CDs fluorescence was in a linear response to the concentration of PPi in the range of 1–200 μM (Fig. 5b). The linear regression equation is $F=30.07C_{PPi}+249.8$ (μM) with a correlation coefficient of 0.9967 ($n=5$). The relative standard deviation obtained (RSD) was 3.06 % for 1.0 and 1.15 % for 200 μM PPi, respectively ($n=7$), demonstrating an excellent precision of the proposed fluorescence system. The limit of detection (LOD) was obtained as 0.32 μM according to the recommendation of IUPAC as $3.29 S_B/m$ which derived from the Orange Book in The Analytical Division, where S_B and m were the standard deviation of the blank and slope of the calibration graph, respectively. It indicated that the present method is sensitive and has promise in practical applications.

In addition, to investigate the feasibility of the present sensor for PPi detection in real samples, PPi level in water samples was measured which was obtained from an artificial wetland located at Liaocheng University. It was carried out according to the experimental procedure after being pretreated. A standard recovery experiment was carried out with the results summarized in Table 1. As shown in Table 1, the recovery was in the range of 92.7−109.1 %, which was acceptable
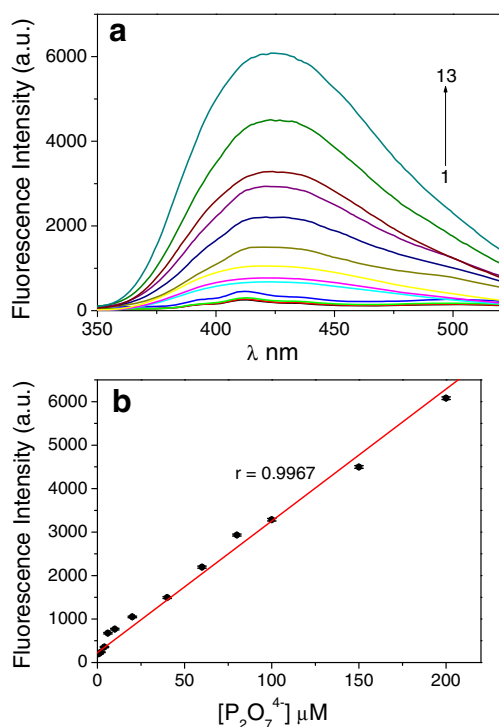
Table 1 Recoveries for the determinations of PPi in water samples from artificial wetland[a]

PPi μM

Sample No.	Content	Added	Found	Recovery ($n=5$, %)	RSD (%)
I	4.27	0	4.23	–	2.37
		5	8.92	96.6	1.65
		10	14.65	103.0	1.68
II	27.51	0	26.32	–	1.29
		10	37.68	92.7	2.01
		20	48.52	109.1	1.94

[a] Conditions: 0.01 mg ml^{-1} CDs, 1 μM Cu^{2+}, Tris–HCl buffer solution, and pH 8.0

for the detection of PPi in the complicated sample. Therefore, the results also showed the practicality and the anti-interference of the present Off-On fluorescence system CDs-Cu^{2+} as a model in trace PPi assay.

Discussion on the Interaction Mechanism of CDs and Metal Ions

The design for the assay of PPi was shown in Scheme 1. It is well known that the fabricated CDs contain plenty of carboxylate moieties on their surface, imparting their excellent water solubility [10]. In the presence of certain metal ions like transition or rare earth metal ions, they coordinate with carboxylate groups on the CDs surface [49], which can induce the aggregation of CDs. On one hand, as a consequence of the aggregating CDs due to transition metal ions such as Cu^{2+}, the fluorescence of CDs is quenched through an energy transfer or other processes. On the other hand, Cu^{2+} can be captured by PPi due to the higher affinity with oxygen-donor atoms from PPi than that with those from the carboxylate groups on the surface of CDs. In this case, the CDs can be disassociated from the coordination reaction with Cu^{2+}, and the fluorescence of CDs can be recovered.

Fluorescence quenching as a useful technique was usually used to obtain adequate information about the structure and dynamics of fluorescent molecules. During the process of fluorescence quenching, the fluorescence intensity of a compound can be decreased by a variety of molecular interactions such as excited-state reaction, molecular rearrangement, energy transfer, forming ground state complex and collisional quenching [50]. Stern-Volmer plots of certain quenching result from static, dynamic or both static and dynamic quenching mode. The static quenching is due to the formation of a non-fluorescent complex between the fluorophore and the quencher in the ground-state, while the dynamic quenching mode is either attributed to the presence of two fluorophores with different accessibility to the quencher and/or attributed to the occurrence of the reverse reaction in the photochemical

Fig. 5 Fluorescence spectra (**a**) and the linear response (**b**) for the detection of pyrophosphate. The *error bars* represent the results of three separate measurements

system [51]. Though there are differences between the static and the dynamic quenching in a way of the sequence of excitation and complex formation, the physical bases of the mechanisms for the two quenching processes are the same.

The two quenching modes can be distinguished by their differing dependence on temperature and viscosity, or preferably by lifetime measurements [52]. On one hand, higher temperatures result in faster diffusion and hence large amounts of collisional quenching. On the other hand, higher temperature will typically result in the dissociation of weakly bound complexes and hence smaller amounts of static quenching. The fluorescence spectra of CDs-Cu^{2+}, CDs-

Fig. 6 Quenching effect of Cu^{2+}, Ni^{2+}, Mn^{2+}, and Co^{2+} ions on the fluorescence spectra of CDs (**a**, **c**, **e**, and **g**) and the Stern-Volmer curves for CDs-Cu^{2+}, CDs-Ni^{2+}, CDs-Mn^{2+}, and CDs-Co^{2+} systems (**b**, **d**, **f**, and **h**) with the concentration range of metal ions of 0–100, 0–600, 0–1, and 0–600 μM, respectively, at room temperature (20 ºC)
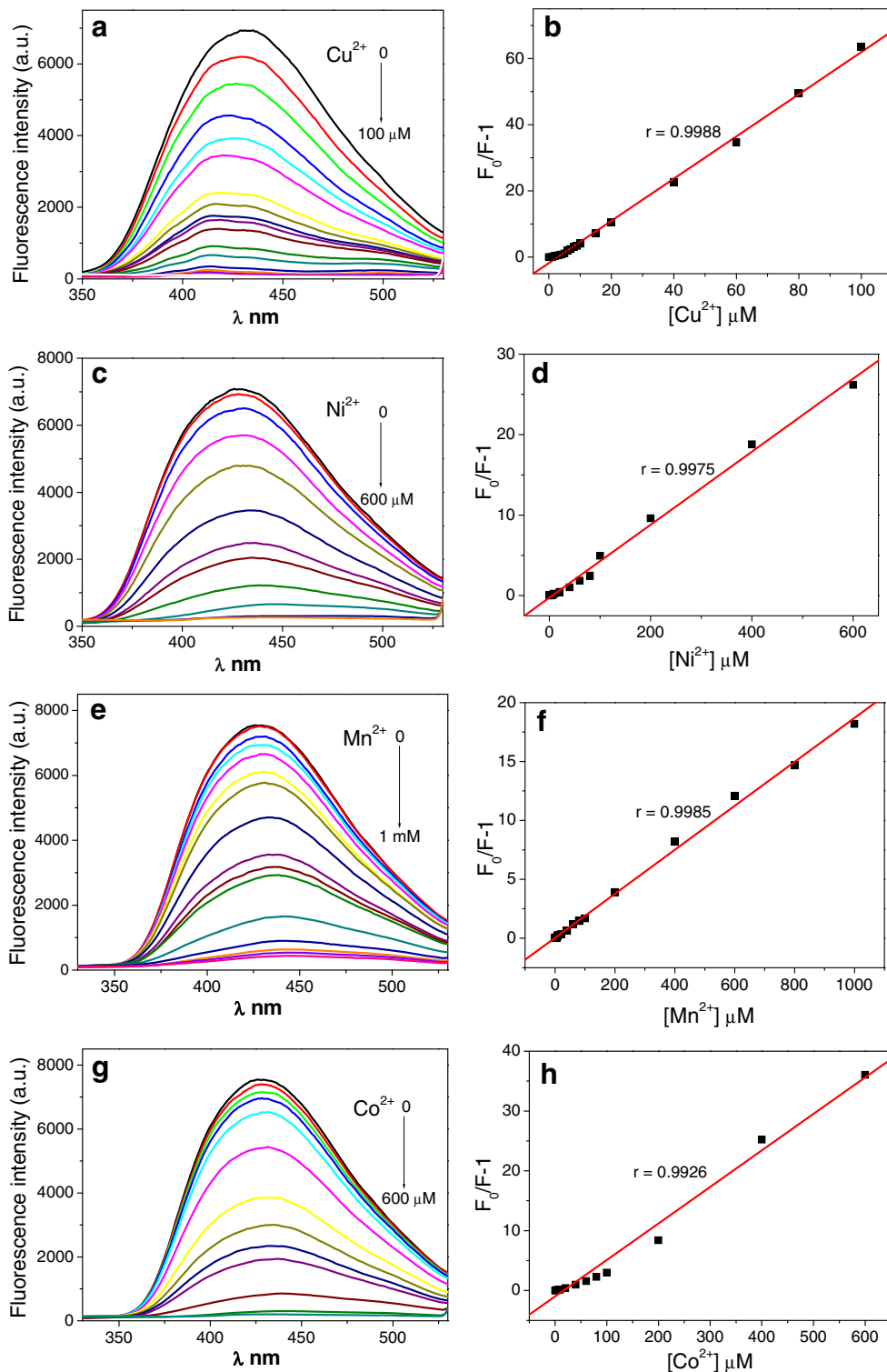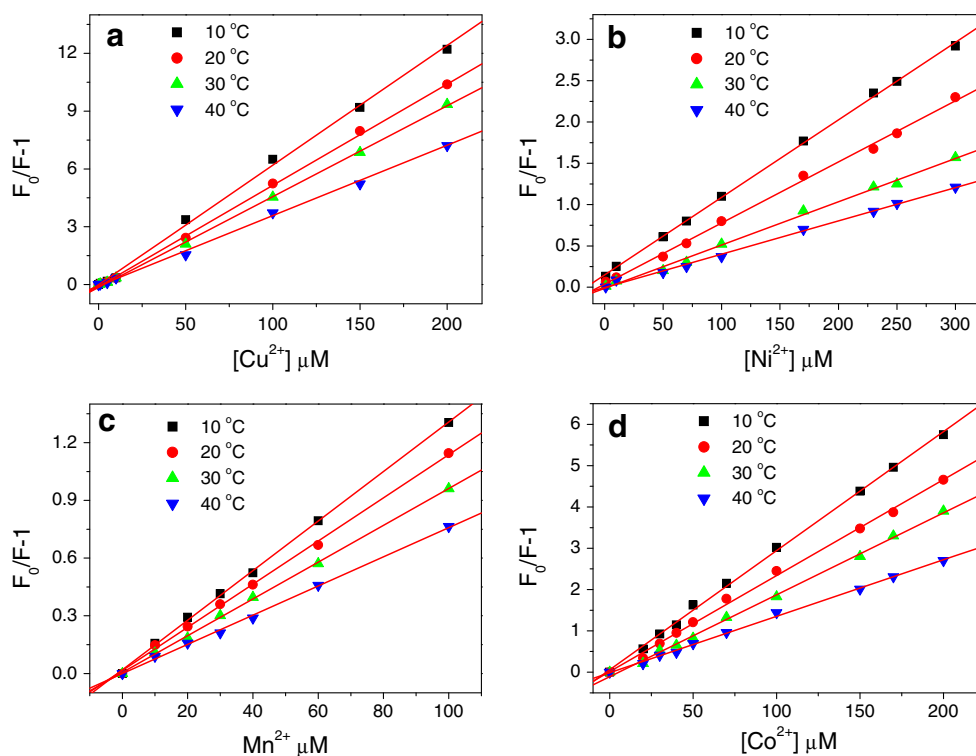
Fig. 7 Stern-Volmer plots of the fluorescence quenching of CDs in aqueous solution by Cu^{2+}, Ni^{2+}, Mn^{2+}, and Co^{2+} under different temperatures

Ni^{2+}, CDs-Mn^{2+}, and CDs-Co^{2+} were illustrated in Fig. 6a, c, e, and g, respectively. It is obvious that the fluorescence intensity of CDs decreases with increasing concentration of all of the tested metal ions and a little wavelength shift on the peak occurred. For the spectra of CDs-Cu^{2+}, there is a little blue-shift, while for spectra of other systems there is a little red-shift with the increasing concentration of metal ions. To some degree, these spectra can also prove the interaction between CDs and metal ions. In addition, it can be easily observed from Fig. 6b, d, f, and h the Stern-Volmer plots for all the tested metal ions are in good linearity and the curve slope decreases with increasing temperature. From the Stern-Volmer plots for all metal ions tested at different temperatures (Fig. 7), it can be deduced that the quenching mode for all metal ions tested is a static quenching procedure. The quenching constants of the four metal ions can be calculated from the Stern-Volmer plots with the results listed in Table 2. It can be found that the quenching effect of the tested metal ions on the fluorescence of CDs is in the order of $Cu^{2+} > Co^{2+} > Mn^{2+} > Ni^{2+}$.

Table 2 Stern-Volmer quenching constants, Ksv, of the CDs-metal ions systems at different temperatures

Metal ion	T (°C)	10^{-5} Ksv (l mol^{-1})	R[a]	RSD%[b]
Cu^{2+}	10	61.88	0.9991	3.16
	20	52.57	0.9998	2.24
	30	47.14	0.9997	1.51
	40	36.02	0.9991	1.28
Ni^{2+}	10	9.39	0.9997	2.80
	20	7.40	0.9988	4.25
	30	5.24	0.9978	4.09
	40	4.03	0.9984	2.68
Mn^{2+}	10	12.88	0.9996	1.34
	20	11.21	0.9993	1.57
	30	9.56	0.9997	1.12
	40	7.59	0.9990	1.24
Co^{2+}	10	28.82	0.9994	3.78
	20	23.24	0.9987	2.56
	30	19.82	0.9990	3.05
	40	13.67	0.9991	2.33

[a] R, linear correlation coefficient
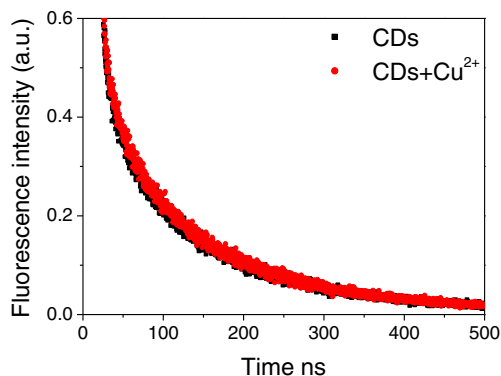
[b] RSD, relative standard deviation

Fig. 8 Fluorescence decay of the CDs as a function of time in the presence of 10 μM Cu^{2+}

In order to further investigate the interaction mechanism of CDs-metal ions and confirm the quenching type of the present system, the lifetime for the excited state of the CDs and CDs-Cu^{2+} (CDs-Cu^{2+} as a model system among the four transition metal ions tested) was also compared (104 ± 0.2 and 103 ± 1.3 ns, respectively, Fig. 8). From the data it can be seen that there is no obvious change for the CDs lifetime in the presence of Cu^{2+}. The results suggested that the fluorescence quenching induced by Cu^{2+} was mainly the static quenching mode due to the formation of non-fluorescent complex, which was accorded with the fact that the surface passivation destruction leading to the fluorescence quenching [38, 39].

Conclusion

In this study, the CDs with the average size of 1.3-nm were synthesized without further modification. The home-made CDs showed strong blue fluorescence with the QY at about 9.9 %, which was higher than those of products prepared by some soot materials. The blue emission of the CDs was quenched heavily by the introduction of some transition metal ions including Cu^{2+}, Ni^{2+}, Mn^{2+} and Co^{2+} due to the combination of the ions and the carboxylic groups on the surface of CDs. In the presence of PPi, the fluorescence for the system of CDs-metal ion was enhanced notably. Based on the Off-On fluorescence system PPi in the water samples from artificial wetland was detected successfully. Compared with currently reported determination methods, our present one displays the advantages of simple, sensitive and cost-effective, avoiding the requirements of sophisticated instruments for the qualitative analysis. Both the previous reports [12–20] and the present result can further confirm a broad range of usage and some potential applications in the analytical and biotechnological fields.

References

1. Wang YH, Shen P, Li CY, Wang YY, Liu ZH (2012) Upconversion fluorescence resonance energy transfer based biosensor for ultrasensitive detection of matrix metalloproteinase-2 in blood. Anal Chem 84:1466
2. Michalet X, Pinaud FF, Bentolila LA et al (2005) Quantum dots for live cells, in vivo imaging, and diagnostics. Science 307:538
3. Kirchner C, Liedl T, Kudera S et al (2005) Cytotoxicity of colloidal CdSe and CdSe/ZnS nanoparticles. Nano Lett 5(2):331
4. Yu P, Wen XM, Toh Y-R, Tang J (2012) Temperature-dependent fluorescence in carbon dots. J Phys Chem C 116:25552
5. Wang X, Cao L, Yang ST et al (2010) Bandgap-like strong fluorescence in functionalized carbon nanoparticles. Angew Chem Int Ed 49(31):5310
6. Baker SN, Baker GA (2010) Luminescent carbon nanodots: emergent nanolights. Angew Chem Int Ed 49(38):6726
7. Xu XY, Ray R, Gu YL et al (2004) Electrophoretic analysis and purification of fluorescent single-walled carbon nanotube fragments. J Am Chem Soc 126(40):12736
8. Li HT, Kang ZH, Liu Y, Lee S-T (2012) Carbon nanodots: synthesis, properties and applications. J Mater Chem 22:24230
9. Wang YL, Anilkumar P, Cao L et al (2011) Carbon dots of different composition and surface functionalization: cytotoxicity issues relevant to fluorescence cell imaging. Exp Biol Med 236:1231
10. Huang J, Deming CP, Song Y, Kang XW, Zhou ZY, Chen SW (2012) Chemical analysis of surface oxygenated moieties of fluorescent carbon nanoparticles. Nanoscale 4:1010
11. Loh KP, Bao QL, Eda G, Chhowalla M (2010) Graphene oxide as a chemically tunable platform for optical applications. Nat Chem 2:1015
12. Li HL, Zhang YW, Wang L, Tian JQ, Sun XP (2011) Nucleic acid detection using carbon nanoparticles as a fluorescent sensing platform. Chem Commun 47(3):961
13. Liu JH, Li JS, Jiang Y, Yang S, Tan WH, Yang RH (2011) Combination of π–π stacking and electrostatic repulsion between carboxylic carbon nanoparticles and fluorescent oligonucleotides for rapid and sensitive detection of thrombin. Chem Commun 47(40):11321
14. Zhou L, Lin YH, Huang ZZ, Ren JS, Qu XG (2012) Carbon nanodots as fluorescence probes for rapid, sensitive, and label-free detection of Hg^{2+} and biothiols in complex matrices. Chem Commun 48(8):1147
15. Shi WB, Wang QL, Long YJ et al (2011) Carbon nanodots as peroxidase mimetics and their applications to glucose detection. Chem Commun 47:6695
16. Zhao HX, Liu LQ, Liu ZD, Wang Y, Zhao XJ, Huang CZ (2011) Highly selective detection of phosphate in very complicated matrixes with an off–on fluorescent probe of europium-adjusted carbon dots. Chem Commun 47:2604
17. Dong YQ, Li GL, Zhou NN, Wang RX, Chi YW, Chen GN (2012) Graphene quantum dot as a green and facile sensor for free chlorine in drinking water. Anal Chem 84:8378
18. Lin Z, Xue W, Chen H, Lin JM (2011) Peroxynitrous-acid-induced chemiluminescence of fluorescent carbon dots for nitrite sensing. Anal Chem 83(21):8245
19. Li HL, Zhai JF, Sun XP (2011) Sensitive and selective detection of silver(I) ion in aqueous solution using carbon nanoparticles as a cheap, effective fluorescent sensing platform. Langmuir 27(8):4305
20. Li HL, Zhai JF, Tian JQ, Luo YL, Sun XP (2011) Carbon nanoparticle for highly sensitive and selective fluorescent detection of mercury(II) ion in aqueous. Biosens Bioelectron 26:4656
21. Huebner PWA, Milburn RM (1980) Hydrolysis of pyrophosphate to orthophosphate promoted by cobalt(III). Evidence for the role of polynuclear species. Inorg Chem 19(5):1267
22. Terkeltaub R (2006) Physiologic and pathologic functions of the NPP nucleotide pyrophosphatase/phosphodiesterase family focusing on NPP1 in calcification. Purinergic Signalling 2:371
23. Ronaghi M, Uhlén M, Nyrén P (1998) A sequencing method based on real-time pyrophosphate. Science 281(5375):363
24. Kim SK, Lee DH, Hong J-I, Yoon J (2009) Chemosensors for pyrophosphate. Acc Chem Res 42(1):23
25. Kruppa M, König B (2006) Reversible coordinative bonds in molecular recognition. Chem Rev 106(9):3520
26. Mikata Y, Ugai A, Ohnishi R, Konno H (2013) Quantitative fluorescent detection of pyrophosphate with quinoline-ligated dinuclear zinc complexes. Inorg Chem 52(18):10223
27. Bhowmik S, Ghosh BN, Marjomäki V, Rissanen K (2014) Nanomolar pyrophosphate detection in water and in a self-

assembled hydrogel of a simple terpyridine-Zn2+ complex. J Am Chem Soc 136(15):5543

28. Credo GM, Su X, Wu K et al (2012) Label-free electrical detection of pyrophosphate generated from DNA polymerase reactions on field-effect devices. Analyst 137(6):1351

29. Villamil-Ramosa R, Yatsimirsky AK (2011) Selective fluorometric detection of pyrophosphate by interaction with alizarin red S–dimethyltin(IV) complex. Chem Commun 47:2694

30. Fabbrizzi L, Marcotte N, Stomeo F, Taglietti A (2002) Pyrophosphate detection in water by fluorescence competition assays: inducing selectivity through the choice of the indicator. Angew Chem Int Ed 41(20):3811

31. Ganjali MR, Hosseini M, Aboufazeli F, Faridbod F, Goldooz H, Badiei AR (2012) A highly selective fluorescent probe for pyrophosphate detection in aqueous solutions. Luminescence 27(1):20

32. Su X, Zhang C, Xiao XJ, Xu AQ, Xu ZD, Zhao MP (2013) A kinetic method for expeditious detection of pyrophosphate anions at nanomolar concentrations based on a nucleic acid fluorescent sensor. Chem Commun 49(8):798

33. Hanshaw RG, Hilkert SM, Jiang H, Smith BD (2004) An indicator displacement system for fluorescent detection of phosphate oxyanions under physiological conditions. Tetrahedron Lett 45(47):8721

34. Liu DJ, Credo GM, Su X et al (2011) Surface immobilizable chelator for label-free electrical detection of pyrophosphate. Chem Commun 47:8310

35. Ray SC, Saha A, Jana NR, Sarkar R (2009) Fluorescent carbon nanoparticles: synthesis, characterization, and bioimaging application. J Phys Chem C 113:18546

36. Tian L, Ghosh D, Chen W, Pradhan S, Chang X, Chen S (2009) Nanosized carbon particles from natural gas soot. Chem Mater 21:2803

37. Lu J, Yang JX, Wang J, Lim A, Wang S, Loh KP (2009) One-pot synthesis of fluorescent carbon nanoribbons, nanoparticles, and graphene by the exfoliation of graphite in ionic liquids. ACS Nano 3:2367

38. Hu SL, Niu KY, Sun J, Yang J, Zhao NQ, Du XW (2009) One-step synthesis of fluorescent carbon nanoparticles by laser irradiation. J Mater Chem 19:484

39. Peng H, Travas-Sejdic J (2009) Simple aqueous solution route to luminescent carbogenic dots from carbohydrates. Chem Mater 21:5563

40. Conry RR (2006) Copper: inorganic & coordination chemistry, Wiley. Encycl Inorg Chem

41. Hu CG, Xiao Y, Zhao Y et al (2013) Highly nitrogen-doped carbon capsules: scalable preparation and high-performance applications in fuel cells and lithium ion batteries. Nanoscale 5(7):2726

42. Zheng HZ, Wang QL, Long YJ, Zhang HJ, Huang XX, Zhu R (2011) Enhancing the luminescence of carbon dots with a reduction pathway. Chem Commun 47:10650

43. Zhu SJ, Meng QN, Wang L et al (2013) Highly photoluminescent carbon dots for multicolor patterning, sensors and bioimaging. Angew Chem Int Ed 52:3953

44. Shi QQ, Li YH, Xu Y et al (2014) High-yield and high-solubility nitrogen-doped carbon dots: formation, fluorescence mechanism and imaging application. RSC Adv 4:1563

45. Fan RJ, Sun Q, Zhang L, Zhang Y, Lu AH (2014) Photoluminescent carbon dots directly derived from polyethylene glycol and their application for cellular imaging. Carbon 71:87

46. Wee SS, Ng YH, Ng SM (2013) Synthesis of fluorescent carbon dots via simple acid hydrolysis of bovine serum albumin and its potential as sensitive sensing probe for lead (II) ions. Talanta 116:71

47. Liu JM, Lin LP, Wang XX et al (2012) Highly selective and sensitive detection of Cu^{2+} with lysine enhancing bovine serum albumin modified-carbon dots fluorescent probe. Analyst 137:2637

48. Ikotun OF, Marino N, Kruger PE, Julve M, Doyle RP (2010) Coordination complexes incorporating pyrophosphate: structural overview and exploration of their diverse magnetic, catalytic and biological properties. Coord Chem Rev 254:890

49. Jiang H, Zhao XY, Schanze KS (2006) Amplified fluorescence quenching of a conjugated polyelectrolyte mediated by Ca^{2+}. Langmuir 22(13):5541

50. Mauricio SM, Holfkens J, Gehlen MH (2008) Static and dynamic biomolecular fluorescence quenching of porphyrin dendrimers in solution. J Fluoresc 18(5):821

51. Htun T (2003) Excited-state proton transfer in nonaqueous solvent. J Fluoresc 13:323

52. Lackowicz JR (1999) Principles of fluorescence spectroscopy, 2nd edn. Kluwer Academic/Plenum Publishers, New York